ARTICLE IN PRESS

Alexandria Engineering Journal (2017) **xxx**, xxx–xxx

HOSTED BY

ELSEVIER

Alexandria University

Alexandria Engineering Journal

www.elsevier.com/locate/aej
www.sciencedirect.com

ORIGINAL ARTICLE

A new hybrid decision tree method based on two artificial neural networks for predicting sediment transport in clean pipes

Isa Ebtehaj, Hossein Bonakdari *, **Amir Hossein Zaji**

Department of Civil Engineering, Razi University, Kermanshah, Iran
Water and Wastewater Research Center, Razi University, Kermanshah, Iran

Received 1 February 2016; revised 13 May 2017; accepted 22 May 2017

KEYWORDS

Artificial Neural Network (ANN);
Decision Tree (DT);
Hybrid model;
Multilayer Perceptron (MLP);
Radial Basis Function (RBF);
Sediment transport

Abstract A new hybrid decision tree (DT) technique based on two artificial neural networks (ANN), namely multilayer perceptron (MLP) and radial basis function (RBF), is proposed to predict sediment transport in clean pipes (i.e. without deposition). The parameters affecting densimetric Froude number (*Fr*) prediction were extracted from the literature in order to build the model proposed in this study. The effect of each parameter is first examined using MLP and RBF and a sensitivity analysis. According to the sensitivity analysis, the optimal model indicates that using the volumetric sediment concentration (C_V), median diameter of particle size distribution to pipe diameter (d/D) and ratio of median diameter of particle size distribution to hydraulic radius (d/R) parameters yield the best *Fr* prediction results. Subsequently, the hybrid DT-MLP and DT-RBF model results are compared with MLP and RBF. According to the results, MLP with all models predicted *Fr* more accurately than RBF, and DT-MLP exhibited the best performance ($R^2 = 0.975$, $MARE = 0.063$, $RMSE = 0.328$, $SI = 00.081$, $BIAS = -0.01$). Moreover, the comparison between DT-MLP and existing regression-based equations indicates that the models presented in the current study are superior.

1. Introduction

For many years engineers have focused on using pipe channels for storm water transfer. The inflow to a pipe channel frequently contains suspended solid substances. Such substances will deposit on the channel bed if the velocity of flow passing through the channel is insufficient or at a certain slope. Sedimentation increases channel bed roughness and decreases the cross-sectional flow area. As a result, the channel's transmission capacity and sediment transport capacity decrease. Consequently, methods of estimating the minimum velocity in a channel to prevent sediment deposition are required.

A traditional method of determining the minimum velocity is to use constant shear stress and velocity [1–3]. This method mostly under or overestimates since the hydraulic conditions

* Corresponding author. Fax: +98 833 428 3264.
E-mail address: bonakdari@yahoo.com (H. Bonakdari).

Peer review under responsibility of Faculty of Engineering, Alexandria University.

http://dx.doi.org/10.1016/j.aej.2017.05.021
1110-0168 © 2017 Faculty of Engineering, Alexandria University. Production and hosting by Elsevier B.V.

Nomenclature

A	cross-sectional area of flow
c	function's center in the nonlinear radial basis function (Eq. (7))
C_V	volumetric sediment concentration
d	median diameter of particle size distribution
D	pipe diameter
Fr	densimetric Froude number
g	gravitational acceleration
k	number of classes in decision tree
p	number of decision tree input variables
R	hydraulic radius
s	specific gravity of sediment ($=\rho_s/\rho$)
S_0	pipe slope
V	flow velocity
V_t	velocity required for the incipient motion of sediment (Eq. (2))
x	input variable in the nonlinear radial basis function (Eq. (7))
y	flow depth

Greek symbols

λ_c	clear water friction factor
λ_s	overall friction factor with sediment
ρ	water density
ρ_s	sediment density

of the flow and channel are not considered [4]. Therefore, numerous researchers have examined the factors affecting minimum velocity determination and presented various equations through experimentation and analyses for estimating sediment transport in clean pipes [5–15]. The clean pipe concept entails sediment transport in a pipe channel without sedimentation occurring on the channel bed.

May et al. [16] carried out 332 tests with 7 experiment sets obtained from Ackers et al. [17] and presented the following semi-experimental equations:

$$C_V = 3.03 \times 10^{-2}\left(\frac{D^2}{A}\right)\left(\frac{d}{D}\right)^{0.6}\left(\frac{V^2}{g(s-1)D}\right)^{1.5}\left(1-\frac{V_t}{V}\right)^4 \quad (1)$$

$$V_t = 0.125[g(s-1)D]^{0.5}\left(\frac{y}{d}\right)^{0.47} \quad (2)$$

where D is the pipe diameter, g is the gravitational acceleration, s is the specific gravity of sediment ($=\rho_s/\rho$), d is the median diameter of particle size distribution, V is the flow velocity, A is the cross-sectional area of flow, C_V is the volumetric sediment concentration, y is the flow depth and V_t is the velocity required for the incipient motion of sediments (Eq. (2)).

Azamathulla et al. [18] employed Ab Ghani [6] and Vongvisessomjai et al.'s [19] datasets to modify Ab Ghani's [6] equation as follows:

$$Fr = \frac{V}{\sqrt{g(s-1)d}} = 0.22C_V^{0.16}D_{gr}^{-0.14}\left(\frac{d}{R}\right)^{-0.29}\lambda_s^{-0.51} \quad (3)$$

where λ_s is the overall friction factor ($\lambda_s = 0.851\lambda_c{}^{0.86}C_V{}^{0.04}$-$\lambda_s = 0.851\lambda_c{}^{0.86}C_V{}^{0.04}D_{gr}{}^{0.03}$, $\lambda_c =$ *clear water friction factor*).

Ebtehaj et al. [20] performed a wide range of experiments using three experimental datasets [6,19,21] and presented an equation for predicting the densimetric Froude number (Fr). The equation is dependent on the volumetric sediment concentration (C_V) and ratio of median diameter of particle size distribution to hydraulic radius (d/R) as follows:

$$Fr = \frac{V}{\sqrt{g(s-1)d}} = 4.49C_V^{0.21}\left(\frac{d}{R}\right)^{-0.54} \quad (4)$$

Because regression-based equations produce different results in different hydraulic conditions, and they are not sufficiently flexible for application in certain hydraulic conditions [14]. Artificial intelligence methods are an alternative means of reducing the inaccuracies of regression-based models and have consequently been widely utilized in diverse engineering sciences, such as hydrology and hydraulic engineering [13,22–27].

Han et al. [28] applied support vector machines (SVMs) in flood forecasting. The authors indicated that the optimum selection of various input combinations is an actual challenge in SVM modeling. Bhattacharya et al. [29] used machine learning methods, artificial neural networks and model trees for bed load and total load modeling using measured data. They compared their model results with existing methods. According to the results, machine learning methods lead to superior modeling accuracy over existing methods. Tirelli and Pessani [30] applied ANN and decision trees to model the presence/absence of telestes muticellus in Northwest Italy. El-Baroudy et al. [31] compared three data-driven methods (evolutionary polynomial regression (EPR), genetic programming (GP) and artificial neural networks (ANN)) in evapotranspiration process modeling. The results demonstrated that EPR is a simpler method with more accurate results than GP and ANN. Senthil Kumar et al. [32] applied different soft computing methods including ANN with backpropagation (BP), radial basis function (RBF), decision trees (DT) such as the REP tree and M5, and fuzzy logic (FL) to predict the suspended sediment concentration upstream of the Bhakra reservoir in North India. Their results indicated that the M5 tree model is more accurate than the other methods. This model also presents decision-makers with a better outlook compared with the rest of the models and offers engineers explicit expressions for practical use. Ebtehaj and Bonakdari [33] examined the performance of two evolutionary algorithms, i.e. the imperialist competitive algorithm (ICA) and genetic algorithm (GA) in predicting the bed load in a clean pipe. These two algorithms were employed to optimize the MLP neural network weights. The results signified that both algorithms predict sediment transport well, although ICA is more accurate than GA. Ebtehaj et al. [34] examined PSO algorithm performance in radial basis function (RBF) neural network (RBF-PSO) training and compared the results with the backpropagation (BP) algorithm. According to their results, prediction accuracy is greater with RBF-PSO than RBF-BP.

In this study, the minimum velocity required to prevent sediment deposition, which is expressed as the densimetric Froude number (Fr), is predicted by means of a novel hybrid method comprising ANN and a decision tree (DT-ANN). The functional equation presented by Ebtehaj and Bonakdari [32] and two different neural networks are initially used to conduct sensitivity analysis on the multilayer perceptron (MLP) and radial basis function (RBF) to determine the effect of each parameter, after which the optimal model is selected. The best model is ultimately used to predict Fr using the two decision tree-integrated neural network models (DT-MLP and DT-RBF). The optimal model's results are then compared with RBF and MLP as well as with regression-based equation results.

2. Data collection

The data employed in this research were obtained from the studies of Ab Ghani [6], Ota and Nalluri [21] and Vongvisessomjai et al. [19], who conducted experiments on pipes with different diameters and lengths. Ab Ghani [6] carried out smooth bed experiments on pipes with diameters of 154, 305 and 450 mm. The roughness was examined on 20.5 m long pipes with 305 mm diameter, and 1.34 mm and 0.53 mm roughness. Ota and Nalluri [21] experimented on a 25 m long pipe with 225 mm diameter to examine the effect of sediment aggregation on sediment transport at limit of deposition. In their experiments, Manning's roughness coefficient, the pipe slope and bed roughness were 0.01, 0.00315 and 0.24 mm respectively. Vongvisessomjai et al. [19] conducted experiments on 16 m long pipes with Manning's roughness coefficient of 0.0125 and diameters of 100 and 150 mm. The hydraulic parameter ranges for the datasets employed are as follows: $0.237 < V$ (m/s) < 1.216; $1 < C_V$ (ppm) < 1280; $0.2 < d$ (mm) < 8.3; $0.012 < R$ (m) < 0.1138; $0.02 < y < 0.229$; $0.000507 < S_0 < 0.006$. The three datasets were used for different hydraulic conditions.

3. Numerical methods

3.1. Multilayer perceptron neural network

Owing to the flexible structure of MLP in simulating nonlinear complex problems [34], this method is one of the most common among neural networks. Each MLP model consists of an input layer, one or more hidden layers, and an output layer. MLP layers comprise neurons. The numbers of input and output layer neurons are equal to the numbers of problem input and output variables, respectively. There is no definitive rule for determining the number of hidden layer neurons, and hence trial and error appears to be a good choice [35–37]. The hidden and output layer neurons collect the previous layer neurons' weights by weighted summation and transfer the weights to the next layer via activation functions. MLP models employ sigmoid activation functions. Each bounded function with a direct relation between input and output variables is a sigmoid function [38]. In this study, the hyperbolic tangent and linear activation functions are used for the hidden and output layers, respectively. These functions are defined as follows:

$$linear(x) = x \tag{5}$$

$$tanh(x) = \frac{2}{1 + e^{-2x}} - 1 \tag{6}$$

As mentioned previously, the MLP method undergoes weighted summation. The process of determining these weights is called training. The MLP models are trained by applying the Levenberg-Marquardt (LM) method [39]. In the LM procedure, the weights and biases are determined using the back-propagation algorithm. The termination criterion for MLP training entails reaching 100 epochs, when the model completely converges.

3.2. Radial basis function neural network

The structure of the RBF neural network [40–41] is quite similar to that of MLP. RBF comprises three types of layers: input, hidden and output layers. The function of the input layer is to introduce the input variables to the model. Subsequently, the experimental dimensionality is reduced by applying a nonlinear projection to the hidden layer using a radial basis function. A real value function whose output is only dependent on the distance from the origin is called a radial basis function [42]. In a nonlinear radial basis function $\varphi(x, c)$, x and c are the input variable and the function's center, respectively. Therefore, any variation in this function is only dependent on the radial distance, which is defined as follows:

$$r = \|x - c\| \tag{7}$$

Upon RBF neural network activation, an N-dimensional function is selected from the linear space as follows [43]:

$$\{\varphi(||x - x_i||)|i = 1, 2, \ldots, N\} \tag{8}$$

Finally, the output layer acts as a linear regressor to prepare the results by doing a weighted summation of the hidden layer's radial basis functions. The weight of this regression is determined with the linear least squares method as follows:

$$f(x) = \sum_{i=1}^{N} c_i \varphi(||x - x_i||) \tag{9}$$

Similar to the MLP method, there is no defined principle for determining the number of RBF hidden layer neurons. Therefore, trial and error [35] is employed in this study.

3.3. Hybrid decision tree-based neural networks

Two hybrid methods, namely DT-MLP and DT-RBF are introduced in this section. The DT algorithm [44] is combined with the MLP and RBF neural networks in order to increase the individual methods' performance. DT is a classification problem with a number of variables. Class variable Y has a value between 1 and k, where k is the number of classes determined for the problem. Output classification is done using input variables X_1 to X_p, where p is the number of input variables. The classification model's goal is to predict the Y value for each new sample of X. In the classification tree, recursive partitioning is applied in order to use one X variable at a time; thus, presenting the DT results become very easy. For instance, a two-variable model with three classes is shown in Fig. 1. The dataset in a two-dimensional graph with its divisions is shown in the left plot, and the corresponding decision tree structure with its splits is shown in the right plot. As seen in this figure, the benefit of a decision tree is that there is no limitation on the input variables; however, the limitation in the left plot is that

Please cite this article in press as: I. Ebtehaj et al., A new hybrid decision tree method based on two artificial neural networks for predicting sediment transport in clean pipes, Alexandria Eng. J. (2017), http://dx.doi.org/10.1016/j.aej.2017.05.021

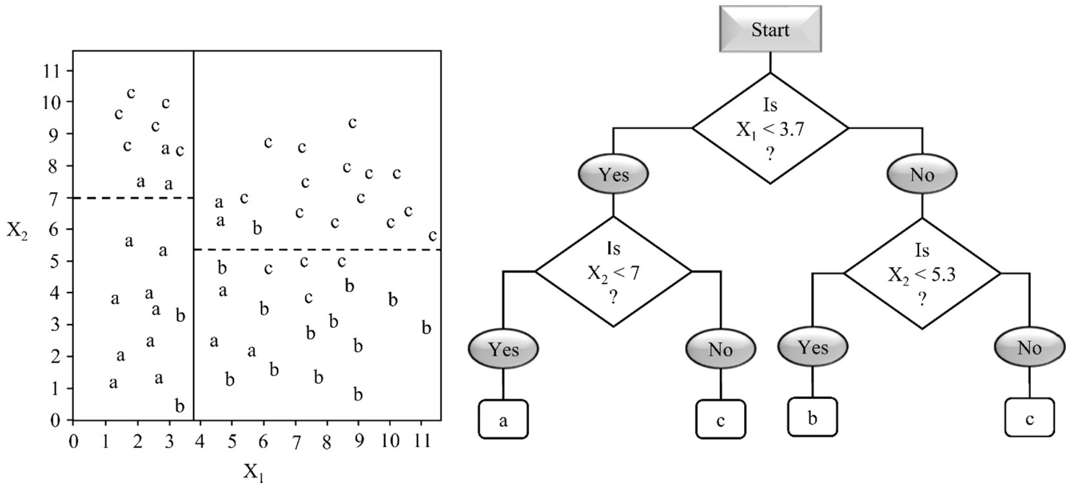

Figure 1 Partitions (the left plot) versus decision tree (the right plot) structures.

there are two input variables at most. Breiman [44] introduced the DT algorithm and its structure in detail.

DT-based hybrid neural networks are optimized in power allocation. Therefore, rather than assigning the entire neural network power to a dataset, the dataset is first partitioned into parts among which the neural network power is divided. The procedure takes place as follows:

(1) DT algorithm training: the DT algorithm is trained using the training input and output variables. In the present study, the entire dataset is divided into four parts. The most important point in DT training is classification precision. Weak classification gives the advantage of a simple DT structure and the disadvantage of high classification error. On the other hand, stronger classification gives the advantage of high accuracy and the disadvantages of a complex DT structure and overtraining. Therefore, trial and error is employed in this study to identify the optimum DT structure accuracy. The Minimum Number of Samples (MNS) of each DT node undergoes trial and error to obtain permission to split. Evidently, increasing the MNS leads to higher classification error and lower DT structure complexity. The optimum MNS obtained in this study is 60.
(2) Neural network splitting: the neural networks are split into smaller models. In this case, the maximum allowable number of hidden layer neurons in the neural networks is considered to be 12. DT divides the dataset into four groups, therefore the maximum allowable number of hidden layer neurons for each group is 12/4 = 3.
(3) Determining the optimum number of hidden layer neurons: trial and error is applied to determine the optimum number of simple neural networks (with a maximum allowable number of 12) and separated neural networks (with a maximum allowable number of 3 for each model).
(4) Result collection: the separated neural networks' outputs are cumulated in order to obtain the final results of the DT-based methods.

Finally, the simple neural network results are compared with the DT-based neural network results to assess the performance of the hybrid methods presented.

4. Methodology

Studies conducted in the field of sediment transport in pipe channels name the following factors that affect sediment transport at limit of deposition: flow velocity (V), volumetric sediment concentration (C_V), flow depth (y) or hydraulic radius (R), pipe diameter (D), median diameter of particle size distribution (d), specific gravity of sediment ($s = \rho_s/\rho$), gravitational acceleration (g) and overall friction factor of sediment (λ_s) [16,18–20]. Therefore, velocity can be written as a functional equation (Eq. (10)) to determine the minimum velocity required to prevent sediment deposition:

$$V = f(C_V, y, R, D, d, s, g, \lambda_s) \tag{10}$$

In order to produce models for predicting sediment transport using ANN and DT, Ebtehaj and Bonakdari [33] presented various dimensionless parameters as shown in Fig. 2. In this figure, the parameters that influence sediment transport are placed in five groups: sediment, transport, transport mode, flow resistance, and movement. Four parameters are used to predict the densimetric Froude number ($Fr = V/(g(s-1)d)^{0.5}$), which is related to the "movement" dimensionless group, and one parameter is selected from each group. The "transport" and "flow resistance" groups only include one parameter. Therefore, the C_V and λ_s parameters are constant in all conditions. With reference to the ratio of median diameter of particle size distribution to pipe diameter (d/D) and dimensionless particle number ($D_{gr} = d(g(s-1)/v^2)^{1/3}$) parameters from the "sediment" group and the d/R, D^2/A and R/D parameters from the "transport mode" group, Ebtehaj and Bonakdari [33] proposed six different models to examine the effect of each parameter. It was found that Model D is the best. Accordingly, the effect of each parameter in model D is examined in this research using sensitivity analysis of the multilayer perceptron (MLP) and radial basis function (RBF) neural networks (Models D1 to D5). Upon selecting

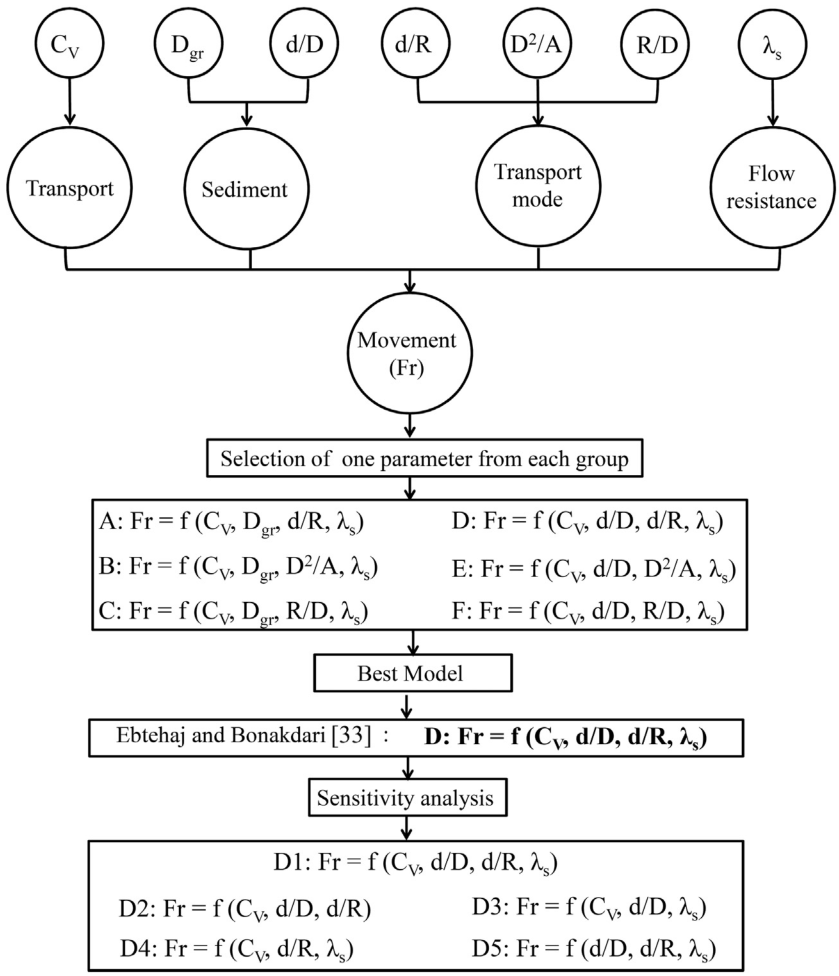

Figure 2 Dimensionless groups and related models.

the optimum model through sensitivity analysis (D1 to D5), the DT-MLP and DT-RBF models are presented by combining DT with the MLP and RBF neural networks. The DT-based dataset separation results are given in Fig. 3. As seen in this figure, DT separates the entire dataset into four groups according to the C_V, d/D, d/R and λ_s input variables. In this study, 70% of all experimental samples comprise the training dataset and the remaining samples comprise the testing dataset.

5. Results and discussion

The results of the MLP, RBF, DT-MLP, and DT-RBF artificial intelligence methods are explained in this section along with the regression-based equations. R-squared (R^2), root mean squared error ($RMSE$), mean absolute relative error ($MARE$), scatter index (SI) and $BIAS$ are used to examine the performance of the models presented in this study. These indices are calculated as follows:

$$R^2 = \left[\frac{\sum_{i=1}^{n}(Fr_{Observed\ i} - \overline{Fr_{Observed}})(Fr_{Predicted\ i} - \overline{Fr_{Predicted}})}{\sqrt{\sum_{i=1}^{n}(Fr_{Observed\ i} - \overline{Fr_{Observed}})^2 \sum_{i=1}^{n}(Fr_{Pedicted\ i} - \overline{Fr_{Predicted}})^2}}\right]^2 \quad (11)$$

$$RMSE = \sqrt{\frac{1}{n}\sum_{i=1}^{n}(Fr_{Observed\ i} - Fr_{Predicted\ i})^2} \quad (12)$$

$$MARE = \frac{1}{n}\sum_{i=1}^{n}\frac{|Fr_{Observed\ i} - Fr_{Predicted\ i}|}{Fr_{Observed\ i}} \quad (13)$$

$$SI = \frac{RMSE}{\overline{Fr_{Observed}}} \quad (14)$$

$$BIAS = \frac{1}{n}\sum_{i=1}^{n}(Fr_{Observed\ i} - Fr_{Predicted\ i}) \quad (15)$$

Table 1 presents the results of the sensitivity analysis conducted using the MLP and RBF neural networks for Model D, which appears to exhibit the best performance among the six models in Fig. 2 [33]. Compared to the other models, D1, D2 and D4 produced the best R^2 with both MLP and RBF. The value of R^2 exceeds 0.95 for MLP with these models and is over 0.85 for RBF (in training). It can be stated that parameters λ_s (Model D2) and d/D (Model D4) are less effective in estimating Fr than parameters C_V and d/R. Excluding λ_s increases $MARE$ by 0.044 for MLP and decreases it by 0.05 for RBF. Not only does neglecting this parameter have a negative effect on the two neural networks' performance, but all the statistical indices presented in Table 1 indicate that Model D2

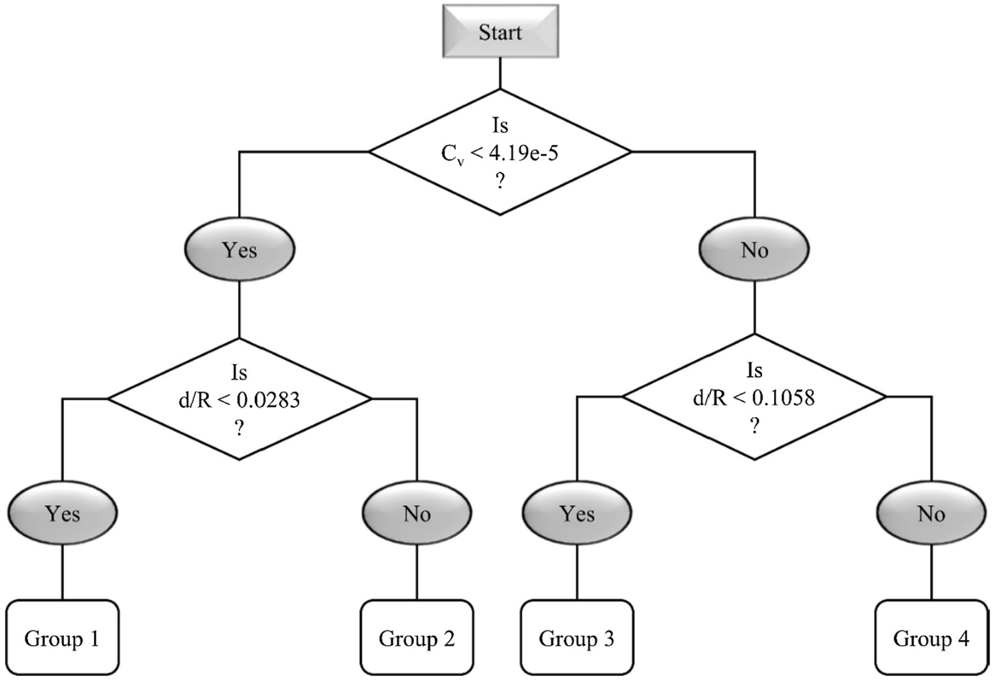

Figure 3 Optimum DT structure.

Table 1 Sensitivity analysis of Model D by MLP and RBF neural networks.

		Train					Test				
		Model D1	Model D2	Model D3	Model D4	Model D5	Model D1	Model D2	Model D3	Model D4	Model D5
MLP	R^2	0.965	0.974	0.889	0.950	0.825	0.950	0.957	0.781	0.869	0.660
	MARE	0.059	0.051	0.123	0.068	0.153	0.076	0.072	0.168	0.116	0.228
	RMSE	0.360	0.310	0.645	0.434	0.810	0.461	0.434	0.980	0.928	1.190
	SI	0.089	0.076	0.159	0.107	0.200	0.114	0.107	0.242	0.229	0.294
	BIAS	0.004	0.010	−0.001	0.000	0.001	−0.070	0.029	−0.204	−0.242	−0.079
RBF	R^2	0.850	0.872	0.819	0.859	0.790	0.807	0.842	0.767	0.815	0.668
	MARE	0.130	0.112	0.147	0.126	0.177	0.171	0.128	0.186	0.165	0.216
	RMSE	0.749	0.692	0.822	0.727	0.886	0.918	0.842	0.993	0.903	1.176
	SI	0.185	0.171	0.203	0.179	0.218	0.227	0.208	0.245	0.223	0.291
	BIAS	0.000	0.000	0.000	0.000	0.000	−0.173	−0.176	−0.140	−0.217	−0.090

outperforms Model D1. Model D2 has a *BIAS* of nearly 0 for both RBF and MLP in training mode, signifying that both methods produce similar average overestimation and underestimation values. However, the *BIAS* value for MLP in testing is positive, indicating overestimation, while this value for RBF is negative, signifying model underestimation. With both RBF and MLP methods, the weakest performance was observed when parameter C_V was omitted in estimating *Fr* (Model D5). The relative error value with MLP tripled for Model D5 compared with Model D1, reaching 22%. RBF presented similar results to MLP with this model. Omitting parameter d/R (Model D3) also affected the results significantly. The mean relative error increased by 4% on average for both methods. It is worth noting that the *MARE* index is almost half the value for Model D5 (MLP), which indicates that parameter C_V has a greater effect on *Fr* estimation than parameter d/R. This is quite similar to RBF where for D4/D5 the *MARE* index is 0.76, which is larger than with MLP. Table 1 additionally indicates that not using parameter λ_s in predicting Fr ($=f(C_V, d/D, d/R)$) decreases the prediction performance and also enhances the MLP and RBF behaviors. Therefore, the performance of D2 (the optimal model recognized in this study) is examined using the decision trees (DT) with MLP and RBF hybrid methods.

Fig. 4 displays the performance results obtained for the hybrid DT-MLP and DT-RBF models in testing and training. The DT-MLP model predicted *Fr* with less than 10% relative error for all data in training. It is also clear that DT-MLP both underestimated and overestimated parameter *Fr*. In testing, this model presented similar results to training, whereby it made most estimations with less than 10% relative error. The DT-RBF model was similar to DT-MLP in training, except it estimated a lot of samples with over 10% relative error. DT-RBF produced similar results in both training and

Please cite this article in press as: I. Ebtehaj et al., A new hybrid decision tree method based on two artificial neural networks for predicting sediment transport in clean pipes, Alexandria Eng. J. (2017), http://dx.doi.org/10.1016/j.aej.2017.05.021

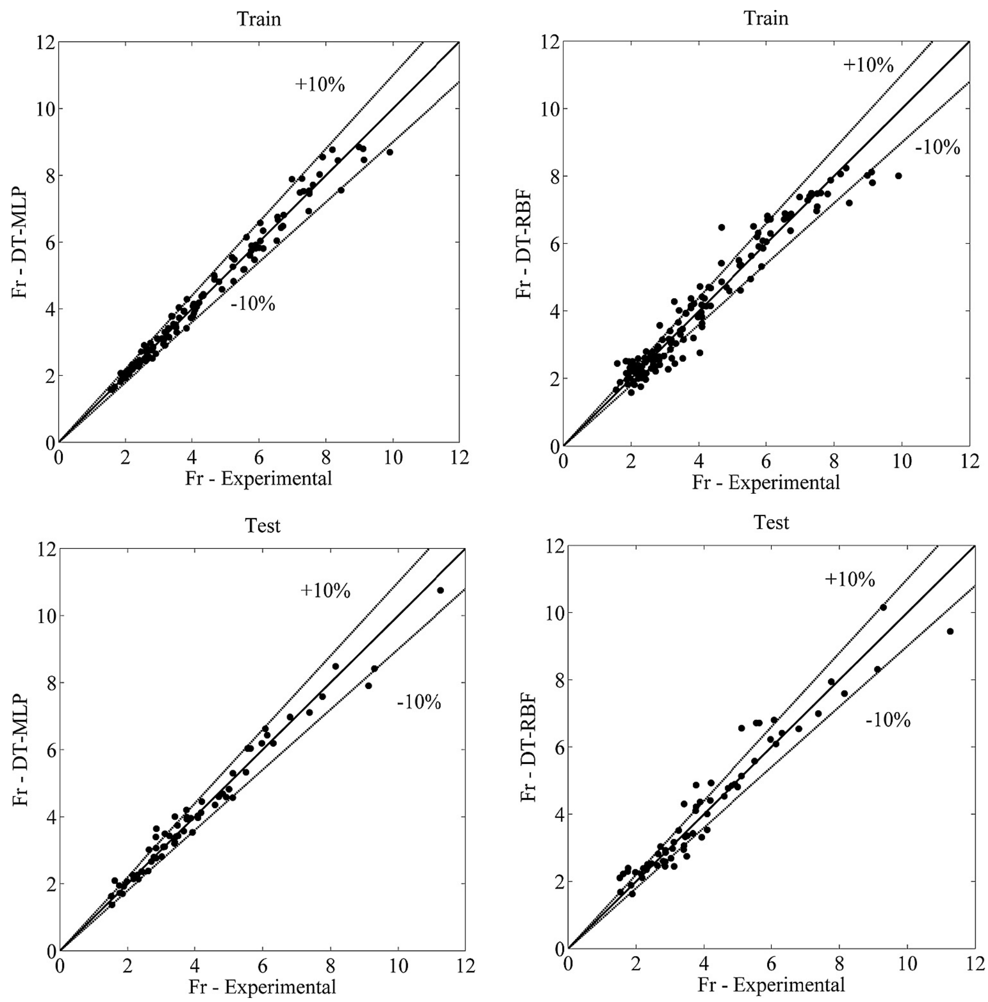

Figure 4 Performance evaluation of DT-MLP and DT-RBP in prediction of *Fr*.

Table 2 Comparison of neural network (MLP and RBF) and hybrid method (DT-MLP and DT-RBF).

		R^2	*MARE*	*RMSE*	*SI*	*BIAS*
Train	MLP	0.974	0.051	0.310	0.076	0.010
	DT-MLP	0.983	0.038	0.255	0.063	0.000
	RBF	0.872	0.112	0.692	0.171	0.000
	DT-RBF	0.943	0.090	0.461	0.114	0.000
Test	MLP	0.957	0.072	0.434	0.107	0.029
	DT-MLP	0.975	0.063	0.328	0.081	−0.010
	RBF	0.842	0.128	0.842	0.208	−0.176
	DT-RBF	0.934	0.103	0.527	0.130	−0.071

testing, signifying this model is flexible in different conditions in terms of the sample type used in model training. However, it is obvious DT-RBF is qualitatively less accurate than DT-MLP in predicting *Fr*.

Table 2 evaluates the performance of two neural networks (MLP and RBF) compared to the DT hybrid models (DT-MLP and DT-RBF) in terms of various statistical indices. It is notable in the table that the hybrid models (DT-MLP and DT-RBF) are more accurate than MLP and RBF in both training and testing. This finding is more significant for the RBF results. For DT-RBF the R^2 values increased by approximately 10% in both testing and training and the relative error values decreased. The *BIAS* value indicates prediction underestimation and overestimation. Regarding Table 2, the *BIAS* value is close to 0 for both methods based on MLP in testing and training. Therefore, this made underestimations and overestimations with an almost equal ratio on average, while RBF and DT-RBF produced negative values that indicate underestimations. The statistical index results for DT-MLP are better than the other models in Table 2. Thus, model D2 that made predictions using DT-MLP is selected as the superior model in this study. The full results of the estimation of all models are presented in Table A1 in Appendix A. The output equation of this model is as follows:

$$Fr = linear((tanh(input \times iw + b_1)) \times lw + b_2) \qquad (16)$$

where the input matrix is $[C_V, d/D, d/R]$, the linear and *tanh* functions are defined as Eqs. (5) and (6) and the iw, lw, b_1 and b_2 matrices for different groups are as follows:

if $C_V < 4.195\text{e}{-05}$ and $d/R < 0.0283$

$$iw = \begin{bmatrix} -20197 & 56569 & 94863 \\ 76 & 120 & 5 \\ 48 & 331 & 68 \end{bmatrix} \quad lw = \begin{bmatrix} -16.7899 \\ -1.2344 \\ 4.6675 \end{bmatrix}$$

$$b_1 = \begin{bmatrix} 0.9063 \\ -2.5878 \\ 0.0491 \end{bmatrix}^T \quad b_2 = [17.1329] \qquad (16.1)$$

if $C_V < 4.195\text{e}{-05}$ and $d/R \geq 0.0283$

$$iw = \begin{bmatrix} -5171 & 38173 \\ 7 & 84 \\ -19 & 54 \end{bmatrix} \quad lw = \begin{bmatrix} -5.519 \\ -0.5988 \end{bmatrix} \qquad (16.2)$$

$$b_1 = \begin{bmatrix} 0.6534 \\ -4.7619 \end{bmatrix}^T \quad b_2 = [5.9252]$$

if $C_V \geq 4.195\text{e}{-05}$ and $d/R < 0.1058$

$$iw = \begin{bmatrix} -509.9 & 2965.3 & 1560.6 \\ 15.3 & 3.8 & 90.9 \\ 14.5 & 15.9 & -65.7 \end{bmatrix} \quad lw = \begin{bmatrix} -5.1292 \\ 243.9365 \\ -4.708 \end{bmatrix}$$

$$b_1 = \begin{bmatrix} -0.1084 \\ 2.3676 \\ -0.6486 \end{bmatrix}^T \quad b_2 = [-231.68] \qquad (16.3)$$

if $C_V \geq 4.195\text{e}{-05}$ and $d/R \geq 0.1058$

$$iw = \begin{bmatrix} 69.6 & 3399.6 & -2003.7 \\ 28.6 & -62.4 & -0.7 \\ 289 & 69.1 & 29 \end{bmatrix} \quad lw = \begin{bmatrix} -0.3983 \\ 0.5292 \\ -1.2313 \end{bmatrix}$$

$$b_1 = \begin{bmatrix} -14.2133 \\ 4.2775 \\ -0.8807 \end{bmatrix}^T \quad b_2 = [1.2968] \qquad (16.4)$$

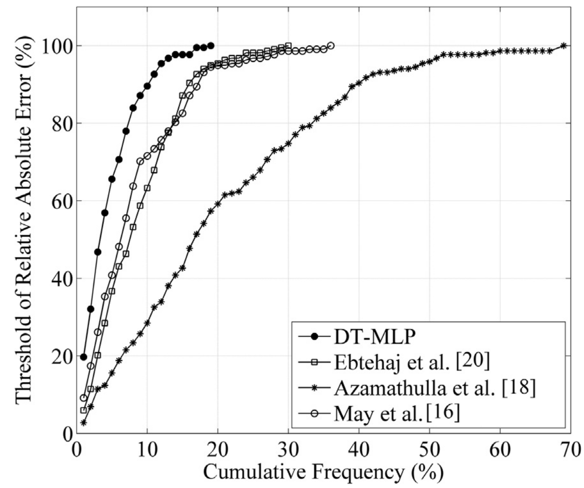

Figure 5 Error distribution of propose method DT-MLP and existing regression-based equation in prediction of *Fr*.

Table 3 compares the DT-MLP results obtained with model D2 with regression-based equations in predicting *Fr* for preventing sediment deposition in pipe channels. May et al. [16] and Ebtehaj et al.'s [20] equations produced values closer to the *MARE*, *RMSE* and *SI* indices than existing regression-based equations. Both equations predicted *Fr* with 8% mean relative error. The R^2 value for Ebtehaj et al.'s [20] equation was superior to that of May et al.'s [16]. This signifies that although May et al.'s [16] equation predicted *Fr* relatively well, it sometimes produced a large relative error in some *Fr* estimations. This problem was also pointed out by Ebtehaj et al. [20]. It can be seen in Fig. 5 that the error distributions of both equations are just about equal, except that the maximum prediction error of Ebtehaj et al.'s [20] equation is lower than May et al.'s [16]. Azamathulla et al.'s [18] equation predicts *Fr* similar to model A (Fig. 2) but performs poorly because the mean relative error is almost 20% ($MARE = 0.2$). Fig. 5 indicates that the maximum prediction error of this model is approximately 70%. This model made only about 35% of the estimations with less than 10% relative error, while the other two regression-based equations made nearly 70% of the estimations with a relative error below 10%. Therefore, the performance of this equation is not satisfactory. Also according to Table 3, DT-MLP, which includes the dimensionless parameters presented in model D2 for predicting *Fr*, outperforms existing equations in terms of all indices. This model produced a mean relative error of approximately 4.5%, which is half the value of Ebtehaj et al.'s [20] equation that performed best among the three existing equations. DT-MLP made roughly 90% of estimations with less than 10% relative error. Moreover, the proposed model had below 20% maximum prediction error, which was nearly 35% for Ebtehaj et al.'s [20] models.

Table 3 Evaluation of proposed model in prediction of *Fr* for Model D2 in comparison with regression-based equation.

Method	R^2	*MARE*	*RMSE*	*SI*	*BIAS*
DT-MLP	0.980	0.045	0.279	0.069	−0.003
May et al. [16]	0.916	0.080	0.574	0.142	−0.050
Azamathulla et al. [18]	0.718	0.200	1.112	0.274	0.295
Ebtehaj et al. [20]	0.967	0.084	0.609	0.150	0.240

Please cite this article in press as: I. Ebtehaj et al., A new hybrid decision tree method based on two artificial neural networks for predicting sediment transport in clean pipes, Alexandria Eng. J. (2017), http://dx.doi.org/10.1016/j.aej.2017.05.021

6. Conclusions

Due to the significance of sediment transport in pipe channels and problems caused by sedimentation, the minimum velocity required for sediment transport in pipe channels so the sediment suspended in the flow passing through pipes does not deposit in the channel was predicted in this study using two hybrid methods. Sensitivity analysis was first conducted using the functional equation presented by Ebtehaj and Bonakdari [33], which appeared to be the best model for predicting sediment transport in pipe channels ($Fr = f(C_V, d/D, d/R, \lambda_s)$), and the MLP and RBF neural networks. Sensitivity analysis was conducted to examine the effect of each dimensionless parameter presented in Ebtehaj and Bonakdari's [33] selected model. The results indicated that excluding the overall friction factor of sediment (λ_s) does not decrease Fr prediction accuracy. The results also demonstrated that excluding parameter C_V has the greatest effect on Fr prediction, since it increased the mean relative error to 20%. Not using parameters d/D and d/R also negatively impacts Fr prediction. Therefore, the superior model selected in this study is $Fr = f(C_V, d/D, d/R)$. Subsequently, the DT-MLP and DT-RBF hybrids comprising two neural networks and decision trees (DT) were compared with MLP and RBF. According to the comparison, DT-MLP ($R^2 = 0.975$, $MARE = 0.063$, $RMSE = 0.328$; $SI = 0.081$; $BIAS = -0.01$) outperformed MLP, while DT-RBF ($R^2 = 0.934$, $MARE = 0.103$, $RMSE = 0.527$; $SI = 0.13$; $BIAS = -0.071$) outperformed RBF. The MLP model was more accurate than RBF in both training and testing. A comparison of the model presented in this article (DT-MLP) with existing regression-based equations further signified that DT-MLP is superior to the existing models.

Appendix A. Datasets

See Table A1.

Table A1 Datasets employed to predict sediment transport in clean pipes.

Investigators	Test #	Dimensionless parameters								Fr				
		λ_s	C_V	D_{gr}	d/R	R/D	y/D	d/D	D^2/A	Observed	MLP	RBF	DT-MLP	DT-RBF
Ab Ghani [6]	1	0.024	426	23.52	0.03	0.23	0.43	0.006	3.06	6.08	6.59	7.33	6.62	6.80
Ab Ghani [6]	2	0.019	151	23.52	0.02	0.25	0.49	0.006	2.64	5.86	5.58	5.07	5.48	5.32
Ab Ghani [6]	3	0.025	186	50.59	0.07	0.19	0.33	0.013	4.38	2.76	2.80	2.78	2.98	2.88
Ab Ghani [6]	4	0.025	309	50.59	0.06	0.22	0.41	0.013	3.26	3.39	3.77	3.67	3.78	3.67
Ab Ghani [6]	5	0.023	164	106.23	0.11	0.24	0.48	0.027	2.66	2.04	2.02	2.09	2.13	2.51
Ab Ghani [6]	6	0.038	285	106.23	0.16	0.17	0.31	0.027	4.89	1.75	1.85	2.44	1.95	2.30
Ab Ghani [6]	7	0.027	163	106.23	0.20	0.14	0.24	0.027	7.12	1.52	2.10	2.44	1.63	2.11
Ab Ghani [6]	8	0.024	1237	144.17	0.17	0.22	0.42	0.037	3.21	2.45	2.71	2.55	2.45	2.16
Ab Ghani [6]	9	0.022	296	23.52	0.02	0.26	0.52	0.006	2.43	6.72	6.15	6.57	6.48	6.38
Ab Ghani [6]	10	0.016	38	23.52	0.02	0.30	0.76	0.006	1.57	4.21	4.71	4.64	4.45	4.93
Ab Ghani [6]	11	0.019	82	23.52	0.02	0.28	0.63	0.006	1.93	5.27	5.54	4.88	5.48	5.36
Ab Ghani [6]	12	0.021	115	50.59	0.05	0.29	0.65	0.013	1.86	3.51	3.55	3.07	3.43	3.36
Ab Ghani [6]	13	0.020	291	50.59	0.05	0.26	0.52	0.013	2.42	4.07	4.08	3.97	4.10	3.96
Ab Ghani [6]	14	0.023	155	50.59	0.05	0.27	0.56	0.013	2.22	3.45	3.58	3.17	3.54	3.42
Ab Ghani [6]	15	0.019	121	50.59	0.05	0.28	0.60	0.013	2.02	3.45	3.49	3.04	3.41	3.33
Ab Ghani [6]	16	0.020	138	106.23	0.09	0.29	0.68	0.027	1.76	2.31	2.31	2.38	2.40	2.02
Ab Ghani [6]	17	0.023	373	106.23	0.11	0.26	0.53	0.027	2.37	2.92	2.71	2.46	2.66	3.15
Ab Ghani [6]	18	0.019	369	144.17	0.12	0.30	0.74	0.037	1.61	2.18	2.41	2.64	2.18	2.36
Ab Ghani [6]	19	0.020	197	11.63	0.01	0.13	0.21	0.002	8.31	8.36	8.54	7.93	8.44	8.24
Ab Ghani [6]	20	0.020	222	24.53	0.03	0.13	0.21	0.003	8.32	5.78	6.05	5.79	5.90	5.92
Ab Ghani [6]	21	0.019	232	24.53	0.02	0.14	0.23	0.003	7.34	5.98	6.25	6.13	6.19	6.23
Ab Ghani [6]	22	0.020	80	24.53	0.02	0.14	0.24	0.003	6.73	4.66	5.24	4.85	5.01	5.42
Ab Ghani [6]	23	0.016	734	24.53	0.02	0.17	0.29	0.003	5.21	9.30	8.46	11.77	8.42	10.16
Ab Ghani [6]	24	0.015	388	24.53	0.02	0.19	0.34	0.003	4.25	9.12	7.09	8.77	7.91	8.31
Ab Ghani [6]	25	0.016	183	24.53	0.02	0.19	0.34	0.003	4.22	7.38	6.90	6.72	7.11	6.99
Ab Ghani [6]	26	0.014	27	24.53	0.01	0.24	0.46	0.003	2.87	5.51	5.37	5.72	5.33	5.58
Ab Ghani [6]	27	0.018	294	50.59	0.04	0.15	0.27	0.007	5.99	4.81	4.73	4.59	4.81	4.70
Ab Ghani [6]	28	0.018	503	50.59	0.04	0.17	0.30	0.007	5.16	6.00	6.18	6.47	5.83	6.06
Ab Ghani [6]	29	0.016	202	50.59	0.03	0.19	0.34	0.007	4.21	5.24	4.85	4.45	4.83	4.61
Ab Ghani [6]	30	0.017	121	50.59	0.03	0.19	0.34	0.007	4.18	4.21	4.24	3.79	4.19	4.15
Ab Ghani [6]	31	0.017	70	50.59	0.03	0.20	0.36	0.007	3.92	3.62	3.78	3.46	3.73	3.93
Ab Ghani [6]	32	0.013	33	50.59	0.03	0.23	0.43	0.007	3.11	3.25	3.50	3.48	3.43	3.52
Ab Ghani [6]	33	0.017	9	50.59	0.03	0.25	0.51	0.007	2.47	2.85	3.04	3.60	3.40	2.45
Ab Ghani [6]	34	0.019	566	144.17	0.12	0.16	0.27	0.019	5.94	2.82	2.87	2.49	2.81	2.55
Ab Ghani [6]	35	0.018	461	106.23	0.09	0.15	0.27	0.014	5.98	3.32	3.26	3.29	3.15	3.04
Ab Ghani [6]	36	0.019	486	106.23	0.09	0.16	0.27	0.014	5.74	3.41	3.43	3.42	3.24	3.06
Ab Ghani [6]	37	0.018	997	106.23	0.08	0.17	0.30	0.014	5.14	4.14	4.13	5.28	4.07	4.15

(*continued on next page*)

Table A1 (*continued*)

Investigators	Test #	Dimensionless parameters								*Fr*				
		λ_s	C_V	D_{gr}	d/R	R/D	y/D	d/D	D^2/A	Observed	MLP	RBF	DT-MLP	DT-RBF
Ab Ghani [6]	38	0.021	43	106.23	0.07	0.19	0.33	0.014	4.37	2.11	2.05	2.13	2.05	2.33
Ab Ghani [6]	39	0.021	7	106.23	0.07	0.19	0.34	0.014	4.25	1.54	1.81	1.99	1.37	1.68
Ab Ghani [6]	40	0.016	308	106.23	0.07	0.19	0.34	0.014	4.21	3.61	4.05	3.98	4.04	3.94
Ab Ghani [6]	41	0.016	903	106.23	0.07	0.19	0.35	0.014	4.10	4.29	4.18	5.76	4.37	4.71
Ab Ghani [6]	42	0.020	14	106.23	0.07	0.21	0.39	0.014	3.55	1.67	1.85	2.01	1.66	1.89
Ab Ghani [6]	43	0.015	52	106.23	0.06	0.24	0.46	0.014	2.84	2.62	2.35	2.27	2.44	2.67
Ab Ghani [6]	44	0.016	17	106.23	0.05	0.25	0.51	0.014	2.49	1.98	2.07	2.13	2.07	2.27
Ab Ghani [6]	45	0.021	418	144.17	0.14	0.14	0.23	0.019	7.14	2.40	2.29	2.42	2.27	2.48
Ab Ghani [6]	46	0.020	196	144.17	0.13	0.14	0.24	0.019	6.75	1.93	2.18	2.35	2.02	2.50
Ab Ghani [6]	47	0.019	566	144.17	0.12	0.16	0.27	0.019	5.94	2.82	2.71	2.91	2.86	3.58
Ab Ghani [6]	48	0.017	1183	144.17	0.11	0.17	0.30	0.019	5.06	3.52	3.46	3.39	3.44	2.60
Ab Ghani [6]	49	0.017	374	144.17	0.10	0.19	0.34	0.019	4.19	3.03	2.90	2.62	2.81	2.69
Ab Ghani [6]	50	0.017	298	144.17	0.10	0.19	0.35	0.019	4.13	2.47	2.69	2.49	2.72	2.55
Ab Ghani [6]	51	0.017	1190	144.17	0.10	0.19	0.35	0.019	4.09	3.67	3.30	4.29	3.57	3.43
Ab Ghani [6]	52	0.016	93	144.17	0.09	0.20	0.36	0.019	3.92	2.14	2.20	2.10	2.19	2.15
Ab Ghani [6]	53	0.014	44	144.17	0.08	0.23	0.43	0.019	3.11	1.90	2.09	2.02	2.03	1.83
Ab Ghani [6]	54	0.014	57	144.17	0.08	0.25	0.49	0.019	2.62	2.24	2.23	2.13	2.19	2.00
Ab Ghani [6]	55	0.020	647	209.93	0.21	0.13	0.21	0.027	8.23	1.95	1.97	1.89	1.95	2.02
Ab Ghani [6]	56	0.019	755	209.93	0.17	0.16	0.27	0.027	5.88	2.32	2.15	2.38	2.28	2.21
Ab Ghani [6]	57	0.016	1280	209.93	0.16	0.17	0.30	0.027	5.17	3.09	3.03	2.14	3.10	2.28
Ab Ghani [6]	58	0.017	144	209.93	0.14	0.20	0.36	0.027	3.90	1.77	1.82	2.19	1.73	2.39
Ab Ghani [6]	59	0.016	1128	209.93	0.13	0.22	0.41	0.027	3.35	3.29	2.92	2.46	3.42	2.45
Ab Ghani [6]	60	0.017	63	209.93	0.13	0.22	0.41	0.027	3.34	1.59	1.78	2.03	1.58	2.45
Ab Ghani [6]	61	0.017	316	209.93	0.12	0.23	0.45	0.027	2.95	2.42	2.30	2.17	2.47	2.48
Ab Ghani [6]	62	0.014	68	209.93	0.11	0.25	0.49	0.027	2.61	1.84	1.82	1.99	1.82	2.51
Ab Ghani [6]	63	0.016	5	18.21	0.01	0.25	0.50	0.002	2.57	5.64	6.41	7.14	6.04	6.71
Ab Ghani [6]	64	0.017	13	18.21	0.01	0.25	0.50	0.002	2.53	7.28	7.62	7.24	7.90	7.40
Ab Ghani [6]	65	0.018	22	18.21	0.01	0.25	0.50	0.002	2.58	9.11	8.75	7.33	8.79	8.12
Ab Ghani [6]	66	0.017	7	18.21	0.01	0.25	0.50	0.002	2.57	6.57	6.30	7.14	6.58	6.82
Ab Ghani [6]	67	0.016	8	18.21	0.01	0.25	0.50	0.002	2.56	7.48	6.87	7.18	6.93	6.97
Ab Ghani [6]	68	0.017	11	18.21	0.01	0.25	0.50	0.002	2.58	8.45	7.28	7.21	7.55	7.20
Ab Ghani [6]	69	0.018	18	18.21	0.01	0.25	0.50	0.002	2.55	9.13	8.28	7.29	8.47	7.81
Ab Ghani [6]	70	0.016	20	18.21	0.01	0.25	0.51	0.002	2.49	9.90	8.61	7.33	8.69	8.01
Ab Ghani [6]	71	0.017	5	18.21	0.01	0.25	0.50	0.002	2.56	6.53	6.42	7.15	6.04	6.72
Ab Ghani [6]	72	0.018	2	18.21	0.01	0.25	0.50	0.002	2.55	4.67	5.97	7.12	4.88	6.48
Ab Ghani [6]	73	0.018	5	18.21	0.01	0.25	0.50	0.002	2.57	5.56	6.41	7.14	6.04	6.71
Ab Ghani [6]	74	0.018	38	18.21	0.01	0.25	0.49	0.002	2.58	11.26	10.54	7.50	10.75	9.44
Ab Ghani [6]	75	0.016	13	18.21	0.01	0.25	0.50	0.002	2.57	6.98	7.58	7.23	7.88	7.38
Ab Ghani [6]	76	0.016	19	18.21	0.01	0.25	0.50	0.002	2.56	7.90	8.39	7.30	8.55	7.88
Ab Ghani [6]	77	0.017	3	18.21	0.01	0.25	0.50	0.002	2.55	5.12	6.12	7.13	5.30	6.56
Ab Ghani [6]	78	0.017	5	18.21	0.01	0.25	0.50	0.002	2.58	6.04	6.40	7.14	6.03	6.71
Ab Ghani [6]	79	0.015	14	18.21	0.01	0.25	0.50	0.002	2.55	7.81	7.74	7.25	8.03	7.47
Ab Ghani [6]	80	0.028	320	24.53	0.02	0.14	0.24	0.003	6.98	6.55	6.73	7.07	6.75	6.89
Ab Ghani [6]	81	0.027	262	24.53	0.02	0.16	0.27	0.003	5.84	6.74	6.58	6.89	6.81	6.88
Ab Ghani [6]	82	0.023	379	24.53	0.02	0.17	0.30	0.003	4.99	7.77	7.05	8.36	7.58	7.94
Ab Ghani [6]	83	0.028	161	50.59	0.04	0.17	0.29	0.007	5.27	3.75	4.10	3.78	4.20	4.11
Ab Ghani [6]	84	0.025	13	50.59	0.03	0.25	0.49	0.007	2.63	2.87	3.13	3.55	3.64	2.86
Ab Ghani [6]	85	0.024	61	50.59	0.03	0.21	0.39	0.007	3.54	3.41	3.84	3.54	3.78	4.02
Ab Ghani [6]	86	0.026	129	50.59	0.03	0.19	0.35	0.007	4.11	3.85	4.35	3.89	4.29	4.22
Ab Ghani [6]	87	0.028	318	50.59	0.04	0.16	0.27	0.007	5.81	4.67	4.94	4.82	4.97	4.87
Ab Ghani [6]	88	0.029	318	50.59	0.06	0.11	0.18	0.007	10.62	3.88	3.53	4.02	3.96	4.37
Ab Ghani [6]	89	0.022	235	50.59	0.03	0.20	0.37	0.007	3.85	5.54	5.22	4.89	5.18	4.95
Ab Ghani [6]	90	0.029	252	106.23	0.08	0.17	0.29	0.014	5.24	2.57	2.74	2.82	2.91	2.68
Ab Ghani [6]	91	0.028	437	106.23	0.10	0.14	0.24	0.014	6.98	3.15	2.89	3.03	2.95	3.41
Ab Ghani [6]	92	0.031	562	106.23	0.12	0.12	0.20	0.014	9.08	2.66	2.78	2.92	2.81	2.62
Ab Ghani [6]	93	0.028	419	106.23	0.09	0.15	0.27	0.014	5.96	3.08	3.11	3.18	3.10	2.98
Ab Ghani [6]	94	0.026	37	106.23	0.06	0.24	0.46	0.014	2.81	2.19	2.21	2.19	2.27	2.14
Ab Ghani [6]	95	0.026	15	106.23	0.06	0.25	0.49	0.014	2.65	1.99	1.99	2.09	1.98	2.21
Ab Ghani [6]	96	0.027	207	106.23	0.07	0.19	0.35	0.014	4.09	2.65	2.89	2.83	3.02	2.82
Ab Ghani [6]	97	0.028	542	106.23	0.09	0.16	0.27	0.014	5.75	3.19	3.63	3.57	3.31	3.15

Table A1 (*continued*)

Investigators	Test #	Dimensionless parameters								*Fr*				
		λ_s	C_V	D_{gr}	d/R	R/D	y/D	d/D	D^2/A	Observed	MLP	RBF	DT-MLP	DT-RBF
Ab Ghani [6]	98	0.030	586	106.23	0.13	0.11	0.18	0.014	10.49	2.65	2.60	2.84	2.55	2.57
Ab Ghani [6]	99	0.022	313	106.23	0.07	0.20	0.36	0.014	3.87	3.84	3.42	3.34	3.42	3.20
Ab Ghani [6]	100	0.029	254	144.17	0.11	0.17	0.29	0.019	5.23	2.20	2.33	2.29	2.34	2.59
Ab Ghani [6]	101	0.029	662	144.17	0.13	0.14	0.24	0.019	6.85	2.65	2.86	2.45	2.66	2.50
Ab Ghani [6]	102	0.027	366	144.17	0.10	0.18	0.33	0.019	4.42	2.80	2.79	2.55	2.76	2.95
Ab Ghani [6]	103	0.030	617	144.17	0.16	0.12	0.20	0.019	9.24	2.32	2.29	2.54	2.33	2.37
Ab Ghani [6]	104	0.029	537	144.17	0.12	0.16	0.27	0.019	5.93	2.63	2.78	2.47	2.74	2.55
Ab Ghani [6]	105	0.025	31	144.17	0.08	0.24	0.46	0.019	2.82	1.89	2.04	2.01	1.93	1.63
Ab Ghani [6]	106	0.030	745	144.17	0.17	0.11	0.18	0.019	10.49	2.27	2.30	2.51	2.35	2.30
Ab Ghani [6]	107	0.023	443	144.17	0.11	0.17	0.30	0.019	4.98	3.20	2.82	2.53	2.91	2.60
Ab Ghani [6]	108	0.027	516	209.93	0.15	0.19	0.33	0.027	4.39	2.30	2.16	2.27	2.27	2.35
Ab Ghani [6]	109	0.032	867	209.93	0.23	0.12	0.20	0.027	9.02	1.88	1.93	1.65	1.87	1.97
Ab Ghani [6]	110	0.029	705	209.93	0.17	0.16	0.27	0.027	5.86	2.15	2.06	2.40	2.26	2.21
Ab Ghani [6]	111	0.025	30	209.93	0.11	0.24	0.46	0.027	2.81	1.56	1.73	1.95	1.59	1.67
Ab Ghani [6]	112	0.029	765	209.93	0.17	0.16	0.28	0.027	8.75	2.25	2.23	2.37	2.30	2.23
Ab Ghani [6]	113	0.032	923	209.93	0.25	0.11	0.18	0.027	10.30	1.85	1.99	1.81	1.71	1.88
Ab Ghani [6]	114	0.025	837	209.93	0.16	0.17	0.31	0.027	4.87	2.59	2.75	2.26	2.52	2.30
Ab Ghani [6]	115	0.024	583	209.93	0.13	0.20	0.37	0.027	3.76	2.66	2.61	2.20	2.65	2.41
Ab Ghani [6]	116	0.028	1	24.53	0.01	0.29	0.68	0.003	1.77	3.30	3.45	5.99	3.18	4.28
Ab Ghani [6]	117	0.021	30	24.53	0.01	0.28	0.61	0.003	1.99	5.63	6.10	6.20	6.14	6.51
Ab Ghani [6]	118	0.029	2	50.59	0.02	0.29	0.68	0.007	1.76	2.28	2.88	3.95	2.31	1.76
Ab Ghani [6]	119	0.023	32	50.59	0.03	0.26	0.54	0.007	2.34	3.41	3.87	3.89	4.01	4.30
Ab Ghani [6]	120	0.025	10	50.59	0.02	0.27	0.56	0.007	2.21	2.87	3.16	3.76	3.49	2.45
Ab Ghani [6]	121	0.023	14	50.59	0.02	0.28	0.63	0.007	1.92	3.10	3.42	3.97	3.75	2.75
Ab Ghani [6]	122	0.023	14	50.59	0.02	0.30	0.72	0.007	1.64	3.04	3.50	4.13	3.77	2.76
Ab Ghani [6]	123	0.025	12	106.23	0.05	0.27	0.56	0.014	2.19	1.97	2.11	2.17	2.18	2.40
Ab Ghani [6]	124	0.024	16	106.23	0.05	0.28	0.63	0.014	1.92	2.14	2.29	2.27	2.36	2.52
Ab Ghani [6]	125	0.022	84	106.23	0.05	0.26	0.54	0.014	2.32	2.75	2.76	2.70	2.75	2.62
Ab Ghani [6]	126	0.022	55	209.93	0.10	0.28	0.59	0.027	2.06	1.78	1.89	2.09	2.09	2.22
Ab Ghani [6]	127	0.038	145	50.59	0.05	0.14	0.24	0.007	6.75	3.97	3.45	3.36	3.73	3.83
Ab Ghani [6]	128	0.034	109	50.59	0.04	0.18	0.31	0.007	4.81	4.06	3.83	3.49	3.87	3.91
Ab Ghani [6]	129	0.032	70	50.59	0.03	0.22	0.41	0.007	3.28	4.08	4.11	3.73	4.01	4.18
Ab Ghani [6]	130	0.027	57	50.59	0.03	0.25	0.51	0.007	2.48	4.60	4.38	4.03	4.35	4.53
Ab Ghani [6]	131	0.038	246	106.23	0.10	0.14	0.25	0.014	6.70	2.72	2.46	2.67	2.67	3.04
Ab Ghani [6]	132	0.035	190	106.23	0.08	0.18	0.31	0.014	4.80	2.79	2.63	2.67	2.79	2.61
Ab Ghani [6]	133	0.032	76	106.23	0.06	0.22	0.41	0.014	3.30	2.82	2.42	2.33	2.52	2.65
Ab Ghani [6]	134	0.033	215	106.23	0.07	0.20	0.35	0.014	4.02	3.16	2.95	2.87	3.07	2.86
Ab Ghani [6]	135	0.038	278	144.17	0.13	0.14	0.24	0.019	6.72	2.34	2.22	2.36	2.14	2.51
Ab Ghani [6]	136	0.035	201	144.17	0.11	0.18	0.31	0.019	4.81	2.40	2.31	2.24	2.33	2.61
Ab Ghani [6]	137	0.032	138	144.17	0.09	0.22	0.41	0.019	3.30	2.43	2.45	2.28	2.46	1.97
Ab Ghani [6]	138	0.026	119	144.17	0.07	0.25	0.51	0.019	2.48	2.72	2.61	2.40	2.56	2.22
Ab Ghani [6]	139	0.033	199	144.17	0.10	0.19	0.35	0.019	3.99	2.72	2.45	2.31	2.53	2.36
Ab Ghani [6]	140	0.039	323	209.93	0.19	0.14	0.25	0.027	6.63	1.91	1.99	2.50	1.93	2.15
Ab Ghani [6]	141	0.036	267	209.93	0.15	0.18	0.31	0.027	4.74	1.96	1.85	2.41	1.93	2.31
Ab Ghani [6]	142	0.033	200	209.93	0.12	0.22	0.41	0.027	3.28	2.00	1.92	2.09	1.95	2.45
Ab Ghani [6]	143	0.034	403	209.93	0.14	0.20	0.36	0.027	3.96	2.21	2.07	2.21	2.20	2.39
Ab Ghani [6]	144	0.030	7	144.17	0.06	0.29	0.65	0.019	1.84	1.91	6.72	7.17	6.66	6.88
Ota and Nalluri [21]	145	0.028	20.4	17.96	0.01	0.19	0.33	0.002	4.34	5.22	5.14	5.86	5.26	5.35
Ota and Nalluri [21]	146	0.026	20.2	17.96	0.01	0.25	0.49	0.002	2.62	6.32	5.72	6.51	6.19	6.41
Ota and Nalluri [21]	147	0.028	25.2	29.85	0.02	0.19	0.33	0.004	4.34	4.05	4.13	4.42	4.15	3.91
Ota and Nalluri [21]	148	0.026	24.9	29.85	0.02	0.25	0.49	0.004	2.62	4.90	4.74	5.23	4.58	4.60
Ota and Nalluri [21]	149	0.030	28.0	50.59	0.04	0.17	0.29	0.007	5.33	2.86	2.64	2.66	2.77	2.93
Ota and Nalluri [21]	150	0.028	28.8	50.59	0.04	0.19	0.33	0.007	4.34	3.11	2.98	2.93	3.12	3.17
Ota and Nalluri [21]	151	0.026	29.7	50.59	0.03	0.22	0.41	0.007	3.27	3.51	3.42	3.36	3.50	3.47
Ota and Nalluri [21]	152	0.026	32.0	50.59	0.03	0.25	0.49	0.007	2.62	3.76	3.76	3.72	3.92	4.16
Ota and Nalluri [21]	153	0.025	27.0	50.59	0.02	0.28	0.62	0.007	1.96	4.09	3.89	4.09	3.97	3.53
Ota and Nalluri [21]	154	0.028	31.5	71.07	0.05	0.19	0.33	0.009	4.34	2.63	2.38	2.32	2.38	2.47
Ota and Nalluri [21]	155	0.026	35.4	71.07	0.04	0.25	0.49	0.009	2.62	3.17	3.20	2.90	3.11	3.05
Ota and Nalluri [21]	156	0.025	29.7	71.07	0.03	0.28	0.62	0.009	1.96	3.45	3.39	3.23	3.49	3.31
Ota and Nalluri [21]	157	0.030	36.3	103.45	0.08	0.17	0.29	0.013	5.33	2.00	2.05	2.01	1.93	1.58

(*continued on next page*)

Please cite this article in press as: I. Ebtehaj et al., A new hybrid decision tree method based on two artificial neural networks for predicting sediment transport in clean pipes, Alexandria Eng. J. (2017), http://dx.doi.org/10.1016/j.aej.2017.05.021

Table A1 (*continued*)

Investigators	Test #	Dimensionless parameters								*Fr*				
		λ_s	C_V	D_{gr}	d/R	R/D	y/D	d/D	D^2/A	Observed	MLP	RBF	DT-MLP	DT-RBF
Ota and Nalluri [21]	158	0.028	43.5	103.45	0.07	0.19	0.33	0.013	4.34	2.18	2.18	2.11	2.15	2.11
Ota and Nalluri [21]	159	0.026	45.4	103.45	0.06	0.22	0.41	0.013	3.27	2.46	2.43	2.31	2.36	2.53
Ota and Nalluri [21]	160	0.026	43.2	103.45	0.05	0.25	0.49	0.013	2.62	2.63	2.67	2.48	2.51	2.80
Ota and Nalluri [21]	161	0.025	41.3	103.45	0.05	0.28	0.62	0.013	1.96	2.86	3.01	2.76	3.07	2.58
Ota and Nalluri [21]	162	0.028	57.7	141.89	0.10	0.19	0.33	0.018	4.34	1.86	1.96	2.01	2.08	2.16
Ota and Nalluri [21]	163	0.026	59.4	141.89	0.08	0.22	0.41	0.018	3.27	2.10	2.14	2.25	2.18	1.82
Ota and Nalluri [21]	164	0.026	57.7	141.89	0.07	0.25	0.49	0.018	2.62	2.25	2.28	2.49	2.27	2.21
Ota and Nalluri [21]	165	0.025	52.1	141.89	0.07	0.28	0.62	0.018	1.96	2.44	2.45	2.80	2.37	2.80
Ota and Nalluri [21]	166	0.028	28.8	50.59	0.04	0.19	0.33	0.007	4.34	3.11	2.98	2.93	3.12	3.17
Ota and Nalluri [21]	167	0.026	29.7	50.59	0.03	0.22	0.41	0.007	3.27	3.51	3.42	3.36	3.50	3.47
Ota and Nalluri [21]	168	0.026	32.0	50.59	0.03	0.25	0.49	0.007	2.62	3.76	3.76	3.72	3.92	4.16
Ota and Nalluri [21]	169	0.025	27.0	50.59	0.02	0.28	0.62	0.007	1.96	4.09	3.89	4.09	3.97	3.53
Ota and Nalluri [21]	170	0.028	29.9	50.59	0.04	0.19	0.33	0.007	4.34	3.11	3.00	2.94	3.11	3.17
Ota and Nalluri [21]	171	0.026	31.2	50.59	0.03	0.25	0.49	0.007	2.62	3.76	3.74	3.71	3.92	4.09
Ota and Nalluri [21]	172	0.025	28.2	50.59	0.02	0.28	0.62	0.007	1.96	4.09	3.93	4.10	3.98	3.63
Ota and Nalluri [21]	173	0.028	29.9	50.59	0.04	0.19	0.33	0.007	4.34	3.11	3.00	2.94	3.11	3.17
Ota and Nalluri [21]	174	0.026	33.9	50.59	0.03	0.22	0.41	0.007	3.27	3.51	3.52	3.40	3.52	3.47
Ota and Nalluri [21]	175	0.026	32.8	50.59	0.03	0.25	0.49	0.007	2.62	3.76	3.78	3.73	3.93	4.22
Ota and Nalluri [21]	176	0.025	30.5	50.59	0.02	0.28	0.62	0.007	1.96	4.09	4.03	4.12	4.01	3.82
Ota and Nalluri [21]	177	0.028	34.1	50.59	0.04	0.19	0.33	0.007	4.34	3.11	3.09	2.97	3.11	3.17
Ota and Nalluri [21]	178	0.026	34.6	50.59	0.03	0.25	0.49	0.007	2.62	3.76	3.83	3.74	3.94	4.37
Ota and Nalluri [21]	179	0.025	32.7	50.59	0.02	0.28	0.62	0.007	1.96	4.09	4.11	4.14	4.03	4.01
Ota and Nalluri [21]	180	0.028	34.1	50.59	0.04	0.19	0.33	0.007	4.34	3.11	3.09	2.97	3.11	3.17
Ota and Nalluri [21]	181	0.026	41.9	50.59	0.03	0.22	0.41	0.007	3.27	3.51	3.70	3.47	3.53	3.47
Ota and Nalluri [21]	182	0.026	40.6	50.59	0.03	0.25	0.49	0.007	2.62	3.76	4.00	3.80	3.99	4.87
Ota and Nalluri [21]	183	0.025	37.7	50.59	0.02	0.28	0.62	0.007	1.96	4.09	4.29	4.19	4.09	4.42
Vongvisessomjai et al. [19]	184	0.048	4	5.06	0.01	0.17	0.30	0.002	5.05	4.17	4.18	5.90	4.14	4.37
Vongvisessomjai et al. [19]	185	0.047	22	5.06	0.01	0.17	0.30	0.002	5.05	5.91	5.63	6.09	5.92	5.86
Vongvisessomjai et al. [19]	186	0.042	24	5.06	0.01	0.25	0.50	0.002	5.05	7.61	7.39	6.94	7.71	7.50
Vongvisessomjai et al. [19]	187	0.053	42	5.06	0.02	0.12	0.20	0.002	5.05	5.73	5.33	5.38	5.60	6.20
Vongvisessomjai et al. [19]	188	0.048	6	7.59	0.02	0.17	0.30	0.003	5.05	3.40	3.60	4.79	3.20	2.95
Vongvisessomjai et al. [19]	189	0.047	29	7.59	0.02	0.17	0.30	0.003	3.41	4.82	4.70	5.02	4.69	4.85
Vongvisessomjai et al. [19]	190	0.041	30	7.59	0.01	0.28	0.60	0.003	3.41	6.66	6.32	6.34	6.43	6.76
Vongvisessomjai et al. [19]	191	0.041	71	7.59	0.01	0.28	0.60	0.003	5.05	8.15	8.61	6.78	8.49	7.59
Vongvisessomjai et al. [19]	192	0.048	6	10.88	0.03	0.17	0.30	0.004	5.05	2.84	3.03	3.71	2.85	2.41
Vongvisessomjai et al. [19]	193	0.047	34	10.88	0.03	0.17	0.30	0.004	3.41	4.03	3.90	3.97	4.08	4.73
Vongvisessomjai et al. [19]	194	0.041	35	10.88	0.02	0.28	0.60	0.004	5.05	5.56	5.40	5.42	5.19	5.63
Vongvisessomjai et al. [19]	195	0.047	79	10.88	0.03	0.17	0.30	0.004	3.41	4.93	4.80	4.38	4.58	4.89
Vongvisessomjai et al. [19]	196	0.041	83	10.88	0.02	0.28	0.60	0.004	5.05	6.81	6.96	5.91	6.98	6.54
Vongvisessomjai et al. [19]	197	0.046	4	5.06	0.01	0.12	0.20	0.001	8.93	4.34	4.53	6.08	4.44	4.68
Vongvisessomjai et al. [19]	198	0.046	21	5.06	0.01	0.12	0.20	0.001	4.37	6.13	5.93	6.26	6.43	6.09
Vongvisessomjai et al. [19]	199	0.041	25	5.06	0.01	0.19	0.33	0.001	8.93	8.19	8.73	7.20	8.77	8.06
Vongvisessomjai et al. [19]	200	0.047	46	5.06	0.01	0.12	0.20	0.001	8.93	7.50	7.42	6.52	7.54	7.48
Vongvisessomjai et al. [19]	201	0.046	5	7.59	0.02	0.12	0.20	0.002	3.41	3.54	3.68	5.01	3.30	3.15
Vongvisessomjai et al. [19]	202	0.038	7	7.59	0.01	0.21	0.40	0.002	3.41	5.19	4.96	6.44	5.54	5.51
Vongvisessomjai et al. [19]	203	0.039	31	7.59	0.01	0.21	0.40	0.002	8.93	7.33	7.26	6.70	7.52	7.49
Vongvisessomjai et al. [19]	204	0.047	57	7.59	0.02	0.12	0.20	0.002	3.41	6.13	5.77	5.53	5.81	6.30
Vongvisessomjai et al. [19]	205	0.039	74	7.59	0.01	0.21	0.40	0.002	3.41	8.98	9.74	7.16	8.85	8.02
Vongvisessomjai et al. [19]	206	0.046	8	10.88	0.02	0.12	0.20	0.003	8.93	2.96	3.25	3.97	3.11	2.67
Vongvisessomjai et al. [19]	207	0.038	9	10.88	0.01	0.21	0.40	0.003	3.41	4.34	4.18	5.57	4.40	4.16
Vongvisessomjai et al. [19]	208	0.039	40	10.88	0.01	0.21	0.40	0.003	3.41	6.13	6.12	5.89	6.34	6.72
Vongvisessomjai et al. [19]	209	0.047	69	10.88	0.02	0.12	0.20	0.003	8.93	5.12	4.82	4.54	4.57	5.14
Vongvisessomjai et al. [19]	210	0.039	90	10.88	0.01	0.21	0.40	0.003	3.41	7.50	7.65	6.41	7.45	7.10
Vongvisessomjai et al. [19]	211	0.041	5	5.06	0.01	0.28	0.60	0.002	3.41	5.76	5.48	6.94	5.74	6.32
Vongvisessomjai et al. [19]	212	0.047	49	5.06	0.01	0.17	0.30	0.002	5.05	7.22	7.18	6.37	7.49	7.28
Vongvisessomjai et al. [19]	213	0.041	6	7.59	0.01	0.28	0.60	0.003	3.41	4.71	4.11	6.09	4.60	4.77
Vongvisessomjai et al. [19]	214	0.047	66	7.59	0.02	0.17	0.30	0.003	5.05	5.90	5.82	5.40	5.81	6.08
Vongvisessomjai et al. [19]	215	0.041	7	10.88	0.02	0.28	0.60	0.004	3.41	3.93	3.66	5.13	3.53	3.31
Vongvisessomjai et al. [19]	216	0.051	37	5.06	0.02	0.08	0.13	0.001	16.06	5.87	5.13	5.38	5.47	5.88
Vongvisessomjai et al. [19]	217	0.046	25	7.59	0.02	0.12	0.20	0.002	8.94	5.01	4.69	5.21	4.82	4.81
Vongvisessomjai et al. [19]	218	0.046	29	10.88	0.02	0.12	0.20	0.003	8.94	4.18	3.93	4.17	4.13	4.41

Please cite this article in press as: I. Ebtehaj et al., A new hybrid decision tree method based on two artificial neural networks for predicting sediment transport in clean pipes, Alexandria Eng. J. (2017), http://dx.doi.org/10.1016/j.aej.2017.05.021

References

[1] American Society of Civil Engineers (ASCE) Water pollution control federation, Design and construction of sanitary and storm sewers, American Society of Civil Engineers Manuals and Reports on Engineering Practices, No. 37, 1970.

[2] British Standard Institution, Sewerage-Guide to New Sewerage Construction, BS8005 Part 1, 1987.

[3] European Standard EN 752–4, Drain and sewer system outside building: Part 4. Hydraulic design and environmental considerations, Brussels: CEN (European Committee for Standardization), 1997.

[4] C. Nalluri, A. Ab, Ghani, Design options for self-Cleansing storm sewers, Water Sci. Technol. 33 (1996) 215–220.

[5] R. Mayerle, C. Nalluri, P. Novak, Sediment transport in rigid bed conveyance, J. Hydraul. Res. 29 (1991) 475–495.

[6] A. Ab Ghani, Sediment Transport in Sewers Ph.D. Thesis, University of Newcastle Upon Tyne, UK, 1993.

[7] D. Butler, R.B. Clark, Sediment management in urban drainage catchments CIRIA Rep. No. 134, CIRIA, London, 1995.

[8] C. Nalluri, F. Spaliviero, Suspended sediment transport in rigid boundary channels at limit deposition, Water Sci. Technol. 37 (1998) 147–154.

[9] R.W.P. May, Preventing sediment deposition in inverted sewer siphons, J. Hhydraul. Eng. 129 (2003) 283–290.

[10] R. Banasiak, Hydraulic performance of sewer pipes with deposited sediments, Water Sci. Technol. 57 (2008) 1743–1748.

[11] J. Almedeij, Rectangular storm sewer design under equal sediment mobility, Am. J. Environ. Sci. 8 (2012) 376–384.

[12] J. Almedeij, N. Almohsen, Remarks on Camp's criterion for self-Cleansing storm sewers, J. Irrig. Drain. Eng-ASCE. 136 (2010) 145–148.

[13] I. Ebtehaj, H. Bonakdari, Bed load sediment transport estimation in a clean pipe using multilayer perceptron with different training algorithms, KSCE J. Civil Eng. 20 (2016) 581–589.

[14] H. Bonakdari, I. Ebtehaj, Verification of equation for non-deposition sediment transport in flood water canals, in: 7th International Conference on Fluvial Hydraulics, RIVER FLOW 2014, Lausanne; Switzerland, 2014, pp. 1527–1533.

[15] I. Ebtehaj, H. Bonakdari, Assessment of evolutionary algorithms in predicting non-deposition sediment transport, Urban Water J. 13 (2015) 499–510.

[16] R.W.P. May, J.C. Ackers, D. Butler, S. Johnt, Development of design methodology for self-cleansing sewers, Water Sci. Technol. 33 (1996) 195–205.

[17] J.C. Ackers, D. Butler, R.W.P. May, Design of Sewers to Control Sediment Problems Report No. 141 CIRIA, Construction Industry Research and Information Association, London, UK, 1996.

[18] H. Azamathulla, A. Ab Ghani, S.Y. Fei, ANFIS – based approach for predicting sediment transport in clean sewer, App. Soft Comput. 12 (2012) 1227–1230.

[19] N. Vongvisessomjai, T. Tingsanchali, M.S. Babel, Non-deposition design criteria for sewers with part-full flow, Urban Water J. 7 (2010) 61–77.

[20] I. Ebtehaj, H. Bonakdari, A. Sharifi, Design criteria for sediment transport in sewers based on self-cleansing concept, J. Zhejiang Univ. Sci-A. 15 (2014) 914–924.

[21] J.J. Ota, C. Nalluri, Graded sediment transport at limit deposition in clean pipe channel, in: 28th International Assoc Hydro-Environ Eng Res, Graz, Austria, 1999.

[22] H. Azimi, H. Bonakdari, I. Ebtehaj, S.H.A. Talesh, D.G. Michelson, A. Jamali, Evolutionary Pareto optimization of an ANFIS network for modeling scour at pile groups in clear water condition, Fuzzy Set. Syst. 319 (2016) 50–69.

[23] S. Ghazanfari-Hashemi, A. Etemad-Shahidi, M.H. Kazeminezhad, A.R. Mansoori, Prediction of pile group scour in waves using support vector machines and ANN, J. Hydroinform. 13 (2011) (2011) 609–620.

[24] H. Sharafi, I. Ebtehaj, H. Bonakdari, A.H. Zaji, Design of a support vector machine with different kernel functions to predict scour depth around bridge piers, Nat. Hazards 84 (2016) 2145–2162.

[25] M. Najafzadeh, G.A. Barani, M.R. HessamiKermani, Estimation of Pipeline Scour due to Waves by GMDH, J. Pipeline Syst. Eng. and Pract. 5 (2014) 06014002.

[26] A.H. Zaji, H. Bonakdari, Application of artificial neural network and genetic programming models for estimating the longitudinal velocity field in open channel junctions, Flow Meas. Instrum. 41 (2015) 81–89.

[27] H. Azimi, H. Bonakdari, I. Ebtehaj, Sensitivity Analysis of the Factors Affecting the Discharge Capacity of Side Weirs in Trapezoidal Channels using Extreme Learning Machines, Flow Meas. Instrum. 54 (2017) 216–223.

[28] D. Han, L. Chan, N. Zhu, Flood forecasting using support vector machines, J. Hydroinform. 9 (2007) 267–276.

[29] B. Bhattacharya, R.K. Price, D.P. Solomatine, Machine learning approach to modeling sediment transport, J. Hydraul. Eng. 133 (2007) 440–450.

[30] T. Tirelli, D. Pessani, Use of decision tree and artificial neural network approaches to model presence/absence of Telestes muticellus in piedmont (North-Western Italy), River Res. Appl. 25 (2009) 1001–1012.

[31] I. El-Baroudy, A. Elshorbagy, S. Carey, O. Giustolisi, D. Savic, Comparison of three data-driven techniques in modelling the evapotranspiration process, J. Hydroinform. 12 (2010) 365–379.

[32] A. Senthil Kumar, C. Ojha, M. Goyal, R. Singh, P. Swamee, Modeling of Suspended Sediment Concentration at Kasol in India Using ANN, Fuzzy Logic, and Decision Tree Algorithms, J. Hydrol. Eng. 17 (2012) 394–404.

[33] I. Ebtehaj, H. Bonakdari, Comparison of genetic algorithm and imperialist competitive algorithms in predicting bed load transport in clean pipe, Water Sci. Technol. 70 (2014) 1695–1701.

[34] S. Haykin, Neural networks: a comprehensive foundation, Prentice Hall PTR, 1994.

[35] O. Kisi, H. Kerem Cigizoglu, Comparison of different ANN techniques in river flow prediction, Civ. Eng. Environ. Syst. 24 (2007) 211–231.

[36] O. Kisi, The potential of different ANN techniques in evapotranspiration modeling, Hydrol. Process. 22 (2008) 2449–2460.

[37] O. Bilhan, E.M. Emiroglu, O. Kisi, Application of two different neural network techniques to lateral outflow over rectangular side weirs located on a straight channel, Adv. Eng. Softw. 41 (2010) 831–837.

[38] M. Smith, Neural networks for statistical modeling, Thomson Learning, 1993.

[39] K. Levenberg, A method for the solution of certain non-linear problems in Least-Squares, Qu. Appl. Math. 2 (1944) 164–168.

[40] D.S. Broomhead, D. Lowe, Radial basis functions, multi-variable functional interpolation and adaptive networks, DTIC Document, 1988.

[41] T. Poggio, F. Girosi, Regularization algorithms for learning that are equivalent to multilayer networks, Sci. 247 (1990) 978–982.

[42] M.D. Buhmann, Radial basis functions: theory and implementations, Cambridge University Press, 2003.

[43] X. Wang, X. Wang, W. Lu, T. Liu, Experimental study on flow behavior at open channel confluences, Front Architect Civ. Eng. China. 1 (2007) 211–216.

[44] L. Breiman, J.H. Friedman, R.A. Olshen, C.J. Stone, Classification and Regression Trees, Chapman & Hall, Boca Raton, 1993.

Please cite this article in press as: I. Ebtehaj et al., A new hybrid decision tree method based on two artificial neural networks for predicting sediment transport in clean pipes, Alexandria Eng. J. (2017), http://dx.doi.org/10.1016/j.aej.2017.05.021